

# Lateral-Current-Injection Type Membrane DFB Laser With Surface Grating

Takahiko Shindo, *Member, IEEE*, Mitsuaki Futami, Tadashi Okumura, *Member, IEEE*, Ryo Osabe, Takayuki Koguchi, Tomohiro Amemiya, *Member, IEEE*, Nobuhiko Nishiyama, *Senior Member, IEEE*, and Shigehisa Arai, *Fellow, IEEE*

**Abstract**—Toward the light source for on-chip interconnection, a current-injection-type membrane distributed feedback laser with a surface grating structure is demonstrated. In this device, 450-nm-thick GaInAsP/InP layers with lateral-current-injection structure prepared by a two step OMVPE regrowth-method is bonded on a host substrate by using Benzocyclobutene bonding process. A threshold current of  $I_{th} = 11$  mA is obtained with a cavity length of 300  $\mu\text{m}$  and a stripe of 1  $\mu\text{m}$ .

**Index Terms**—Semiconductor laser, membrane laser, lateral-current-injection, surface grating structure.

## I. INTRODUCTION

THE progress in the processing speed of the large scale integrated (LSI) circuits is predicted that will soon confront the limitation due to the ohmic heating, RC delay and large power consumption in the global wiring. As one of promising solutions for these problems, a replacement of the electrical global wiring on a chip with an optical interconnection has been proposed [1]. The optical devices for such optical interconnection should have properties of low power consumption and a small footprint. Especially, semiconductor lasers are strongly required to operate with ultra low driving current [1]. VCSEL [2] and microdisk lasers [3] have been reported to be promising devices for low power consumption. Recently, for the light source of the on-chip optical interconnection, an optically pumped photonic crystal laser has been reported with the low power dissipation of 8.76 fJ/bit because of its strong optical confinement effect

[4], [5]. In addition, in recent years, electrically pumped photonic-crystal lasers have been demonstrated [6], [7]. However, they have disadvantages, such as low output, and difficulty in controlling the output efficiency because optical confinement in an extremely small cavity is too strong.

The membrane DFB laser, which we have investigated for the light source of the on-chip optical interconnection, has a thin semiconductor core layer and low refractive-index cladding layers such as SiO<sub>2</sub> or Benzocyclobutene (BCB). Due to its strong optical confinement in vertical direction as well as strongly index-coupled short cavity DFB structure, ultra-low threshold current operation can be expected without sacrificing differential quantum efficiency. Furthermore, toward realization of photonic integrated circuits based on membrane structure, other optical components such as lateral junction waveguide type photodetector [8], low loss GaInAsP photonic wire waveguide [9] and so on were also realized. The compact and low consumption in-plane photonic integrated circuit would be realized using the membrane structure.

In our early works on the membrane laser, ultra low threshold operation has been reported with optical pumping [10], [11]. Furthermore, lateral-current-injection (LCI) structure has been adopted [12] and LCI type lasers on SI-InP substrate have been demonstrated [13], [14] as a step to realize an electrically pumped membrane laser. Recently, first demonstration of current injection type membrane-DFB laser with wirelike active regions had been achieved under room-temperature (RT) pulsed current condition [15]. However, the threshold current was higher than 80 mA and was very high compared with the calculated result.

In this letter, we introduced surface grating structure [16], [17] and demonstrated much lower threshold current operation of the LCI membrane laser.

## II. DEVICE STRUCTURE AND THEORETICAL ANALYSIS

Figure 1 shows a schematic structure of the fabricated LCI-membrane-DFB laser with a surface grating structure, where the total core layer thickness was about 450 nm, and the top and bottom cladding layers were composed of air ( $n = 1$ ) and SiO<sub>2</sub> ( $n = 1.45$ ), respectively. The thin LCI-membrane-structure was fabricated on an InP host substrate by using BCB bonding process. The InP host substrate was used just for easiness of cleavage and changing the host substrate to Si or SOI can be done without any problem for real applications. A surface grating structure was formed on the top of a laser

Manuscript received January 9, 2013; revised March 26, 2013 and April 21, 2013; accepted April 29, 2013. Date of publication May 31, 2013; date of current version June 18, 2013. This work was supported in part by the JSPS KAKENHI under Grants 24246061, 19002009, 22360138, 21226010, 23760305, and 10J08973, in part by the Ministry of Internal Affairs and Communications through SCOPE, and in part by the Council for Science and Technology Policy through FIRST program.

T. Shindo and T. Amemiya are with the Quantum Nanoelectronics Research Center, Tokyo Institute of Technology, Tokyo 152-8552, Japan (e-mail: hindou.t.aa@m.titech.ac.jp; amemiya.t.ab@m.titech.ac.jp).

M. Futami, T. Okumura, R. Osabe, T. Koguchi, and N. Nishiyama, are with the Department of Electrical and Electronic Engineering, Tokyo Institute of Technology, Tokyo 152-8552, Japan (e-mail: futami.m.aa@m.titech.ac.jp; tokumurable@gmail.com; osabe.r.aa@m.titech.ac.jp; koguchi.t.aa@m.titech.ac.jp; n-nishi@pe.titech.ac.jp).

S. Arai is with the Quantum Nanoelectronics Research Center, Tokyo Institute of Technology, Tokyo 152-8552, Japan, and also with the Tokyo Institute of Technology, Quantum Nanoelectronics Research Center, Tokyo 152-8552, Japan (e-mail: arai@pe.titech.ac.jp).

Color versions of one or more of the figures in this letter are available online at <http://ieeexplore.ieee.org>.

Digital Object Identifier 10.1109/LPT.2013.2261980

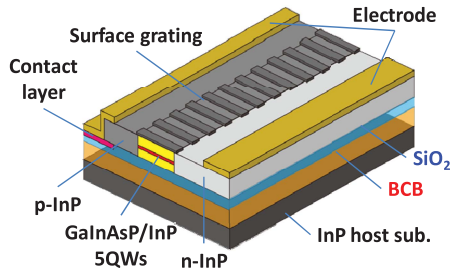


Fig. 1. Schematic device structure of the lateral-current-injection semiconductor membrane laser with surface grating structure.

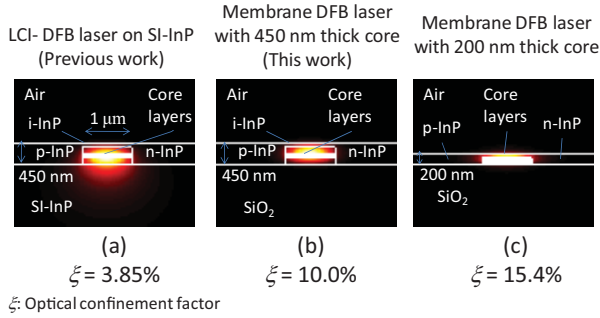


Fig. 2. Cross sectional optical mode field of various LCI type lasers.

stripe by etching a part of the InP cap layer. Due to the high index contrast between the GaInAsP core layer and air or the SiO<sub>2</sub> cladding layer, the optical confinement factor in the active layers and the index coupling coefficient of the surface grating can be enhanced.

Figure 2 shows the comparison of the calculated cross sectional optical mode field in the core layer of the various LCI type lasers. The stripe width of these devices was assumed to be 1  $\mu\text{m}$ , and InP regions were formed at the both sides of the laser stripe. The core layer consists of 5 quantum wells with 6-nm-thick wells and 9-nm-thick barriers sandwiched by GaInAsP optical confinement layers, and a 10-nm-thick undoped InP top layer. Fig. 2 (a) shows LCI-DFB laser on SI-InP substrate we demonstrated previously [17], and Figs. 2(b) and 2(c) show those of membrane lasers with the total core layer thickness of 450 nm and 200 nm, respectively. The estimated optical confinement factor in 5 quantum-wells of the LCI-DFB laser on SI-InP is relatively low value of  $\xi = 3.85\%$ , when the stripe width is  $W_s = 1 \mu\text{m}$ . This is because of asymmetric vertical optical confinement structure (i.e. the upper cladding is air ( $n = 1$ ) and the lower cladding is InP ( $n = 3.17$ )). By adopting the stripe width of 2  $\mu\text{m}$ , the optical confinement factor can be enhanced to be about 5%, however the threshold current becomes higher due to an increase of the volume of the active region. In contrast, an enhancement of the optical confinement factor can be realized in the membrane structure with the low refractive index material of air ( $n = 1$ ) and SiO<sub>2</sub> ( $n = 1.45$ ) to both upper and lower cladding layers, respectively. In this letter, we adopted the total core layer thickness of 450 nm, and the optical confinement factor was estimated to be 10.0%. Furthermore, by adopting the core layer thickness of less than 200 nm, the optical confinement factor can be enhanced to be more than 15%.

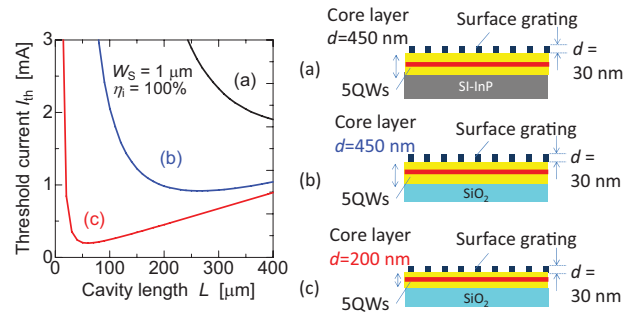


Fig. 3. Calculated threshold current dependence on the cavity length of various LCI type lasers.

Figure 3 shows the calculated threshold current dependence on the cavity length of 3 types of LCI lasers shown in Fig. 2. The threshold current of these devices were calculated by using the coupled wave theory. In this calculation, the internal quantum efficiency was assumed to be 100%. As reduction of core layer thickness, not only the enhancement of the optical confinement in the active region but also the enhancement of the index-coupling coefficient of the grating can be attainable. The estimated coupling coefficient of the structures in Figs. 3(a), 3(b), and 3(c) were  $\kappa = 100 \text{ cm}^{-1}$ ,  $150 \text{ cm}^{-1}$ , and  $1500 \text{ cm}^{-1}$ , respectively. As a result, threshold current less than 1 mA can be realized in the membrane laser with core layer thickness of 450 nm (Fig. 3(b)). This value is around a half of that of the structure we previously demonstrated (Fig. 3(a)). In addition, by the reduction of the core layer thickness to 200 nm, threshold current can be further reduced to 200  $\mu\text{A}$  when the cavity length of about 50  $\mu\text{m}$  is used.

### III. EXPERIMENTAL RESULT

Figure 4 shows the fabrication process of the LCI-membrane laser by using BCB bonding process. An initial wafer, consisting of 1% compressively-strained 5-quantum-wells (CS-5QWs, 6 nm thick) sandwiched by symmetric GaInAsP optical confinement layers (OCLs) and a 50-nm-thick InP cap layer, was prepared by OMVPE method. The LCI structure was formed by two step regrowth method [13]. First, the mesa structure was formed by CH<sub>4</sub>/H<sub>2</sub> reactive ion etching (RIE) process. After removing damaged surface by wet chemical cleaning, n-InP was selectively regrown on both sides of the mesa structure. Next narrow (1- $\mu\text{m}$ ) stripe was formed by etching a part of the mesa structure, p-InP and GaInAs contact layers were regrown in the same way. Then, the membrane structure was formed by using BCB bonding process [9]. After depositing 1  $\mu\text{m}$ -thick SiO<sub>2</sub>, 2  $\mu\text{m}$ -thick BCB was coated on the regrown wafer and a host InP substrate, and the wafer was attached upside down to the host substrate. Therefore, the total thickness of the BCB layer after bonding was expected to be about 4  $\mu\text{m}$ . By using this bonding process, we could obtain the BCB thickness of less than 2  $\mu\text{m}$  [9]. Then the InP substrate and etch stop layers of the regrown wafer were removed by polishing and wet chemical etching. Next, Ti/Au electrodes were deposited on both p-GaInAs contact layer (p-InP side cladding was partially removed to expose this contact layer) and n-InP layer. Finally, the surface grating pattern was formed by electron-beam lithography and CH<sub>4</sub>/H<sub>2</sub>

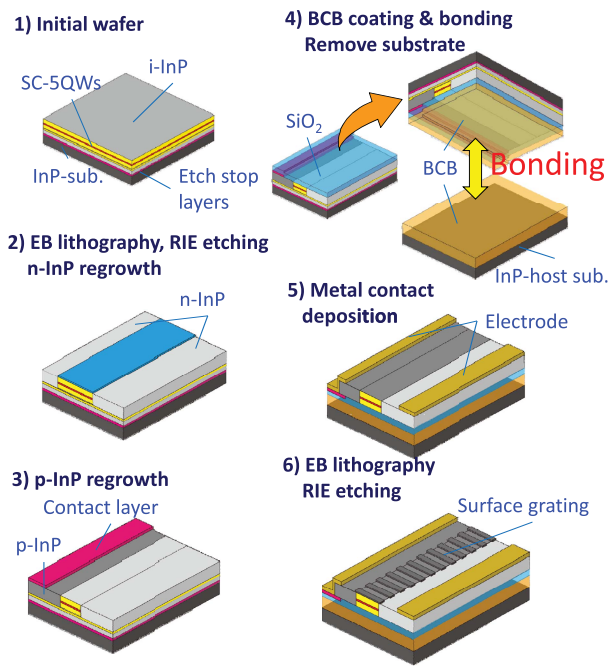


Fig. 4. Fabrication process of LCI-membrane laser by using BCB bonding process.

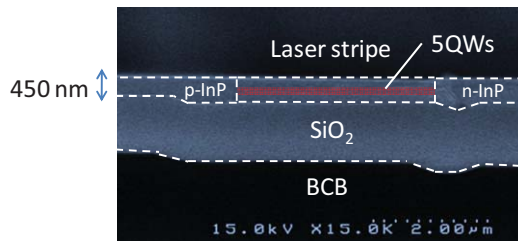


Fig. 5. Cross sectional SEM view of the LCI-membrane structure formed by BCB bonding process.

RIE on the top InP cap layer at the laser stripes. The grating period and the depth were 255 nm and 30 nm, respectively. The index-coupling coefficient of this grating was estimated to be  $\kappa = 150 \text{ cm}^{-1}$ .

Figure 5 shows the SEM view of the fabricated membrane structure, where the membrane structure with core layer thickness of 450 nm was successfully fabricated on the host InP substrate by using BCB bonding process. The estimated BCB thickness was about 4  $\mu\text{m}$ . The upper and lower cladding layers were low refractive index materials of air and  $\text{SiO}_2$ , respectively. In addition, the lateral p-i-n structure was fabricated by forming the p- and n-InP regions at the sides of the core layer, and flat top surface of membrane structure was obtained.

Figure 6 shows a light output and voltage-current characteristics of the LCI-membrane-DFB laser with a surface grating structure under room-temperature pulsed-current condition (1  $\mu\text{s}$ -width, 1 ms-period). The cavity length and the stripe width were  $L = 300\text{-}\mu\text{m}$  and 1- $\mu\text{m}$ , respectively. A threshold current of 11 mA, which was much lower than the previous report was obtained [15], however it was approximately 10 times higher than that of the theoretical value shown in Fig. 3. This might be attributed to low internal quantum efficiency of

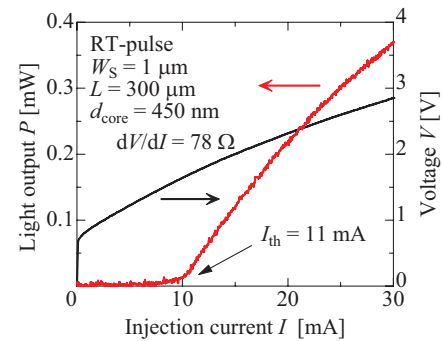


Fig. 6. Lasing characteristics of the fabricated membrane laser with the cavity length of 300  $\mu\text{m}$ .

the LCI type lasers due to non-radiative recombinations at the surface of the core layer. The internal quantum efficiency of the LCI laser on SI-InP was estimated to be about 40% [12]. In case of the LCI-membrane laser, more lower internal quantum efficiency was expected because the membrane structure has two sides to its semiconductor surface (upper and lower sides of the core layer). The differential quantum efficiency of the fabricated device was about 2.5%. This value is less than one-tenth of the estimated  $\eta_d$  of 29% from the coupled wave theory. Therefore, internal quantum efficiency  $\eta_i$  of the fabricated LCI-membrane laser is thought to be less than 10%, and the threshold current is expected to be 9.2 mA. In order to suppress such non-radiative recombination, we already reported some novel core structures suited for LCI-membrane lasers and can expect their highly-efficient operations with  $\eta_i$  of around 70% [16], [17]. Furthermore, poor lasing characteristics are attributed to poor a BCB bonding process since air voids were trapped in the bonding interface which might have resulted in large waveguide loss. In fact, a GaInAsP low loss membrane-wire waveguide has already been demonstrated using special BCB bonding process [9]. Improvements of the BCB bonding technique are also essential. As previously described, the final target of the membrane laser is a realization of ultra-low threshold current operation by enhancing the optical confinement factor and index coupling coefficient. In addition to the improvements of internal quantum efficiency and waveguide loss, introduction of a thinner core layer ( $\sim 200 \text{ nm}$ ) and shorter cavity structure ( $\sim 50 \mu\text{m}$ ) is required toward realization of ultra-low threshold current operation shown in Fig.3

The differential series resistance and the voltage at the threshold were around 78  $\Omega$  and 1.7 V, respectively. Since the rise-up voltage was around 0.8 V and was similar to conventional lasers in 1.5  $\mu\text{m}$  wavelength region, the relatively high threshold voltage is attributed to a higher series resistance which was 3.1 times higher than that of LCI-DFB laser with 400 nm thick core layer prepared on a SI-InP substrate [16]. A continuous-wave operation was not obtained because of heat generation due to the high series resistance. Furthermore, by introducing thin core layer thickness of less than 200 nm and short cavity length of less than 50  $\mu\text{m}$ , the series resistance is expected to increase. In the current device, the distance between the edge of the active region and metal electrode in p-doped InP region was set to be 3  $\mu\text{m}$ . The estimated

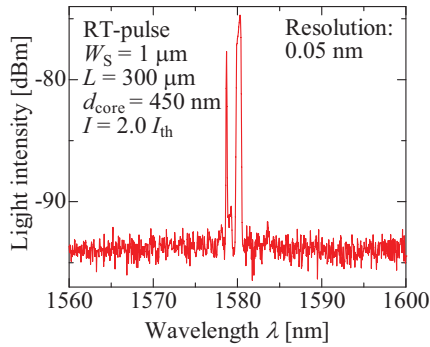


Fig. 7. Lasing spectrum of the fabricated membrane laser at a bias current of two times the threshold current ( $I = 22$  mA).

sheet resistance of this region was  $2.7 \text{ k}\Omega/\square$  with the core thickness of  $400 \text{ nm}$  [14] and this value is more than 100 times larger than that of n-InP region. Therefore, the series resistance of this region can be the dominant factor of the high series resistance of the device. In theory, with assumption of the distance in p-InP region of  $1 \mu\text{m}$ , the series resistance of the membrane laser is expected to be around  $150 \Omega$  when the short cavity of  $50 \mu\text{m}$  and thin core layer thickness of  $200 \text{ nm}$  are adopted. The reduction of the series resistance of the membrane laser is strongly required to realize low power consumption light source.

The thermal resistance of the membrane laser is also expected to be high compared with that of typical semiconductor laser. However, with assumption of ultra-low threshold current operation, the expected self-heating caused by injected current has little effect on the lasing characteristics of the LCI-membrane-DFB laser thanks to its small driving current [20].

Figure 7 shows a lasing spectrum of the membrane DFB laser at two times the threshold. As can be seen, a two mode operation ( $1578.7 \text{ nm}$  and  $1580.3 \text{ nm}$ ) was observed. This two mode operation might be attributed to relatively high  $\kappa L = 4.5$  of the DFB cavity without phase-shift region for the stripe width of  $1 \mu\text{m}$ , and the cavity length of  $300 \mu\text{m}$ .

#### IV. CONCLUSION

In summary, we demonstrated a current injection type semiconductor membrane DFB laser with a core layer thickness of about  $450 \text{ nm}$ , by adopting a surface grating structure using BCB bonding process. The threshold current of  $11 \text{ mA}$  was realized under room-temperature pulsed current condition for the cavity length of  $300 \mu\text{m}$  and the stripe width of  $1 \mu\text{m}$ .

#### ACKNOWLEDGMENT

The authors would like to thank Professors M. Asada, F. Koyama, T. Mizumoto, Y. Miyamoto, M. Watanabe, and Dr. Tadashi Okumura, Tokyo Institute of Technology, for fruitful discussions.

#### REFERENCES

- [1] D. A. B. Miller, "Device requirements of optical interconnects to silicon chips," *Proc IEEE*, vol. 97, no. 7, pp. 1166–1185, Jul. 2009.
- [2] P. Moser, *et al.*, "81 fJ/bit energy-to-data ratio of 850 nm vertical-cavity surface-emitting lasers for optical interconnects," *Appl. Phys. Lett.*, vol. 98, no. 23, pp. 231106-1–231106-3, Jun. 2011.
- [3] D. V. Thourhout, *et al.*, "Nanophotonic devices for optical interconnect," *IEEE J. Sel. Topics Quantum Electron.*, vol. 16, no. 5, pp. 1363–1375, Sep./Oct. 2010.
- [4] S. Matsuo, *et al.*, "High-speed ultracompact buried heterostructure photonic-crystal laser with 13fJ of energy consumed per bit transmitted," *Nature Photon.*, vol. 4, no. 9, pp. 648–654, Aug. 2010.
- [5] S. Matsuo, *et al.*, "20-Gbit/s directly modulated photonic crystal nanocavity laser with ultra-low power consumption," *Opt. Express*, vol. 19, no. 3, pp. 2242–2250, Jan. 2011.
- [6] B. Ellis, *et al.*, "Ultralow-threshold electrically pumped quantum-dot photonic-crystal nanocavity laser," *Nature Photon.*, vol. 24, no. 5, pp. 297–300, May 2011.
- [7] S. Matsuo, *et al.*, "Room-temperature continuous-wave operation of lateral current injection wavelength-scale embedded active-region photonic-crystal laser," *Opt. Express*, vol. 20, no. 4, pp. 3773–9780, Feb. 2012.
- [8] T. Okumura, *et al.*, "Lateral junction waveguide-type photodiode grown on semi-insulating InP substrate," *Jpn. J. Appl. Phys.*, vol. 50, no. 2, pp. 020206-1–020206-3, Feb. 2011.
- [9] J. Lee, Y. Maeda, Y. Takino, N. Nishiyama, and S. Arai, "Low-loss GaInAsP wire waveguide on Si substrate with benzocyclobutene adhesive wafer bonding for membrane photonic circuits," *Jpn. J. Appl. Phys.*, vol. 51, pp. 0402201-1–0402201-5, Mar. 2012.
- [10] S. Sakamoto, *et al.*, "Strongly index-coupled membrane BH-DFB lasers with surface corrugation grating," *IEEE J. Sel. Topics Quantum Electron.*, vol. 13, no. 5, pp. 1135–1141, Sep./Oct. 2007.
- [11] S. Arai, N. Nishiyama, T. Maruyama, and T. Okumura, "GaInAsP/InP membrane lasers for optical interconnects," *IEEE J. Sel. Topics Quantum Electron.*, vol. 17, no. 5, pp. 1381–1389, Sep./Oct. 2011.
- [12] K. Oe, Y. Noguchi, and C. Caneaus, "GaInAsP lateral current injection lasers on semi-insulating substrates," *IEEE Photon. Technol. Lett.*, vol. 6, no. 4, pp. 479–481, Apr. 1994.
- [13] T. Okumura, *et al.*, "Lateral current injection GaInAsP/InP laser on semi-insulating substrate for membrane-based photonic circuits," *Opt. Express*, vol. 17, no. 15, pp. 12564–12570, Jul. 2009.
- [14] T. Okumura, H. Ito, D. Kondo, N. Nishiyama, and S. Arai, "Continuous wave operation of thin film lateral current injection lasers grown on semi-insulating InP," *Jpn. J. Appl. Phys.*, vol. 49, no. 4, pp. 040205-1–040205-3, Apr. 2010.
- [15] T. Okumura, T. Koguchi, H. Ito, N. Nishiyama, and S. Arai, "Injection-type GaInAsP/InP membrane buried heterostructure distributed feedback laser with wirelike active regions," *Appl. Phys. Express*, vol. 4, no. 4, pp. 042101-1–042101-3, Mar. 2011.
- [16] T. Shindo, *et al.*, "GaInAsP/InP lateral-current-injection distributed feedback laser with a-Si surface grating," *Opt. Express*, vol. 19, no. 3, pp. 1884–1891, Jan. 2011.
- [17] T. Shindo, *et al.*, "Lateral-current-injection distributed feedback laser with surface grating structure," *IEEE J. Sel. Topics Quantum Electron.*, vol. 17, no. 5, pp. 1175–1182, Sep./Oct. 2011.
- [18] M. Futami, *et al.*, "Improved quantum efficiency of GaInAsP/InP top air-clad lateral current injection lasers," in *Proc. 1st Opt. Interconnects Conf.*, May 2012, pp. 34–35.
- [19] M. Futami, *et al.*, "GaInAsP/InP lateral current injection laser with uniformly distributed quantum-well structure," *IEEE Photon. Technol. Lett.*, vol. 24, no. 11, pp. 888–891, Jun. 1, 2012.
- [20] K. Doi, *et al.*, "Thermal analysis of self-heating effect in GaInAsP/InP membrane DFB laser on Si substrate," in *Proc. IEEE Photon. Conf.*, Sep. 2012, pp. 814–815.